Supporting information

Unveiling the role of NiFeM hydroxides (M=Pt, Ru, Ir, Rh) cocatalysts for robust H_2 production in photocatalytic water splitting†

Mengmeng Shao,*[ab] Wei Shi,[c] Junhui Jiang,[d] Shihua Tan,[e] Xuehan Wang,[b] Jiawei Fei,[b] Jinhua Li[b] and Zhangjing Zhang*[a]

[a] Fujian Provincial Key Laboratory of Polymer Materials, College of Materials Science and Engineering, Fujian Normal University, Fuzhou 350007, China
Email: shaommzjut@163.com; zzhang@fjnu.edu.cn
[b] Zhejiang Huayuan Pigment Co., Ltd, Huzhou 313220, China
[c] Hangzhou Chaoteng Energy Technology Co., Ltd, Hangzhou 310051, China
[d] Taizhou Pollution Prevention and Control Engineering Center Co., Ltd, Taizhou 318000, China
[e] Hunan Province Key Laboratory of Materials Surface or Interface Science and Technology, Central South University of Forestry and Technology, Changsha 410004, China

This file includes Fig. S1-S15, and Table S1-S5.

1. Experimental section

1.1. Chemicals and materials

Nickel nitrate hexahydrate ($Ni(NO_3)_2 \cdot 6H_2O$), platinum tetrachloride ($PtCl_4$), triethanolamine ($C_6H_{15}NO_3$, TEOA), ethanol were purchased from Shanghai Aladdin Biochemical Technology Co., Ltd. Iron nitrate nonahydrate ($Fe(NO_3)_3 \cdot 9H_2O$), ruthenium trichloride trihydrate ($RuCl_3 \cdot 3H_2O$), rhodium trichloride trihydrate ($RhCl_3 \cdot 3H_2O$), and urea ($CO(NH_2)_2$) were purchased from Shanghai Macklin Biochemical Co., Ltd. Iridium trichloride trihydrate ($IrCl_3 \cdot 3H_2O$) was obtained from Shanghai Bide Pharmatech Ltd. Sodium sulfate (Na_2SO_4), sodium sulfite (Na_2SO_3), sodium sulfide nonahydrate ($Na_2S \cdot 9H_2O$), and potassium hydroxide (KOH) were purchased from Tianjin Damao Chemical Reagent Factory. Nafion solution (5 wt%) was acquired from Shanghai Hesen Electrical Co., Ltd. The above chemicals were of analytical grade and utilized as received. Indium tin oxide (ITO) glass substrates were provided by Nanbo Glass Shenzhen, China. The highly purified water was used in our experiments and produced by a ultrapure water system (ULUPURE, UPR-II-TN).

1.2. Fabrication of Pt group metals doped NiFe-LDH cocatalysts

The NiFe-LDH doped with Pt group metals was fabricated by traditional hydrothermal method. Specifically, for NiFePt-LDH synthesis, 1.5 mmol $Ni(NO_3)_2 \cdot 6H_2O$, 0.5 mmol $Fe(NO_3)_3 \cdot 9H_2O$, 30 mmol urea, and 0.02 mmol $PtCl_4$ were dissolved in 40 mL water. Afterwards, the above solution was transferred to the Teflon-lined autoclave and heated to 120 °C for 12 h. The reaction was then cooled down naturally and the solid product was washed several times with water and

ethanol, which was finally dried at 60 °C for 12 h to obtain the NiFe-LDH with Pt dopant, i.e. NiFePt-LDH. For the synthesis of other noble metal-doped NiFe-LDH, the same process was carried out but replacing $PtCl_4$ with $RuCl_3 \cdot 3H_2O$, $IrCl_3 \cdot 3H_2O$, or $RhCl_3 \cdot 3H_2O$. Herein, the as-prepared NiFeM-LDH (M=Pt, Ru, Ir, Rh) was denoted as NiFeM for simplicity. And the pristine NiFe-LDH was also synthesized through the same approach and denoted as NiFe.

1.3. Fabrication of NiFeM-LDH loaded g-C_3N_4

The NiFeM-LDH loaded g-C_3N_4 was prepared by the ultrasound-assisted self-assembly process. Firstly, the pristine g-C_3N_4 was synthesized by calcining urea at 550 °C for 4 h. Then the received g-C_3N_4 (50 mg) and NiFeM-LDH (10 mg) were dispersed separately in ethanol and sonicated for 30 min. Subsequently, the two suspensions were mixed and further sonicated for another 60 min to acquire NiFeM-LDH loaded g-C_3N_4 after filtration, washing and drying. Herein, the NiFeM-LDH loaded g-C_3N_4 was denoted as NiFeM/CN, and the pristine NiFe-LDH modified g-C_3N_4 was also prepared and recorded as NiFe/CN.

1.4. Material characterizations and photoelectrochemical properties

The as-prepared samples were characterized by X-ray diffractometer (XRD), scanning electron microscopy (SEM), energy dispersive spectrometer (EDS), N_2 adsorption-desorption isotherm, X-ray photoelectron spectroscopy (XPS), ultraviolet photoelectron spectroscopy (UPS), UV-vis diffuse reflectance spectra (UV-vis DRS), and photoluminescence spectroscopy (PL). The XRD patterns were acquired on a Bruker D8 Advance diffractometer with Cu Kα radiation. SEM images and EDS

results were obtained on a FEI Verios G4 UC microscopy. The N_2 adsorption-desorption isotherms were performed by using Quantachrome Autosorb-iQ-MP instrument. XPS and UPS spectra were acquired on a Thermo ESCALAB Xi+ microprobe. UV-vis DRS was performed on an Agilent Cary5000 spectrometer with $BaSO_4$ as reference. PL spectra were obtained on an Edinburgh FLS1000 spectrometer with 325 nm excitation wavelength.

The photoelectrochemical properties were measured on a standard three-electrode system via the CHI760E instrument, where the Hg/HgO and Pt sheet were employed as the reference and counter electrodes, respectively. For the photocurrent and impedance measurements, the photocatalysts were deposited onto ITO (1 cm × 1 cm) as working electrode with a loading amount of 0.25 mg/cm^2, and a mixture of Na_2SO_4 (0.1 M), Na_2SO_3 (0.1 M), and Na_2S (0.01 M) was used as the electrolyte. Specifically, a constant potential of 0.8 V vs Hg/HgO was adopted to detect the photocurrent response of our prepared photocatalysts. The impedance analysis was carried out at the potential of 0.8 V vs Hg/HgO with amplitude of 10 mV and frequency range of 0.1 Hz to 100 kHz. For the HER test, the cocatalysts were deposited onto carbon paper (1 cm × 1 cm) as working electrode with a loading amount of 0.5 mg/cm^2, and 1 M KOH solution was used as the electrolyte.

1.5. Photocatalytic HER measurements

The photocatalytic HER activities of our prepared photocatalysts were evaluated in a sealed reactor with top-illuminated mode under 300 W Xe-lamp light source. Specifically, 15 mg photocatalyst was ultrasonically dispersed in 45 mL solution

containing 10 vol% TEOA as sacrificial agent. Next, the reaction system was purged with Ar for 15 min to remove air and then tightly sealed for photocatalytic reaction. During light irradiation, 0.2 mL of gas was sampled for analysis every hour through gas chromatograph (FULI GC7980 with TCD detector). The apparent quantum efficiency (AQE) was tested in the same way, but a 420 nm bandpass filter was used to acquire the 420 nm monochromatic light with power intensity of 14.5 mW/cm^2. The AQE data was calculated as follows:

$$\mathrm{AQE} = \frac{2 \times \text{Number of produced } \mathrm{H_2}}{\text{Number of incident photons}}$$

2. Computational method

The density functional theory (DFT) calculations were performed by the Vienna ab-initio simulation package (VASP),[1,2] where the exchange-correlation functional was treated by the Perdew-Burke-Ernzerhof (PBE) parametrization of the generalized gradient approximation (GGA).[3-5] For structure relaxation, the 5×1×1 k-point grid was used for Brillouin zone sampling, and a kinetic energy cutoff of 500 eV was employed. Meanwhile, the lattice constants and atom coordinates were both optimized until the force was less than 0.01 eV/Å. The DFT-D3 method was used to describe the van der Waals (vdW) interaction.[6] For the HER simulation, the supercell slab (4×1) of (100) edge containing 4 layers was constructed with a 15 Å vacuum layer.

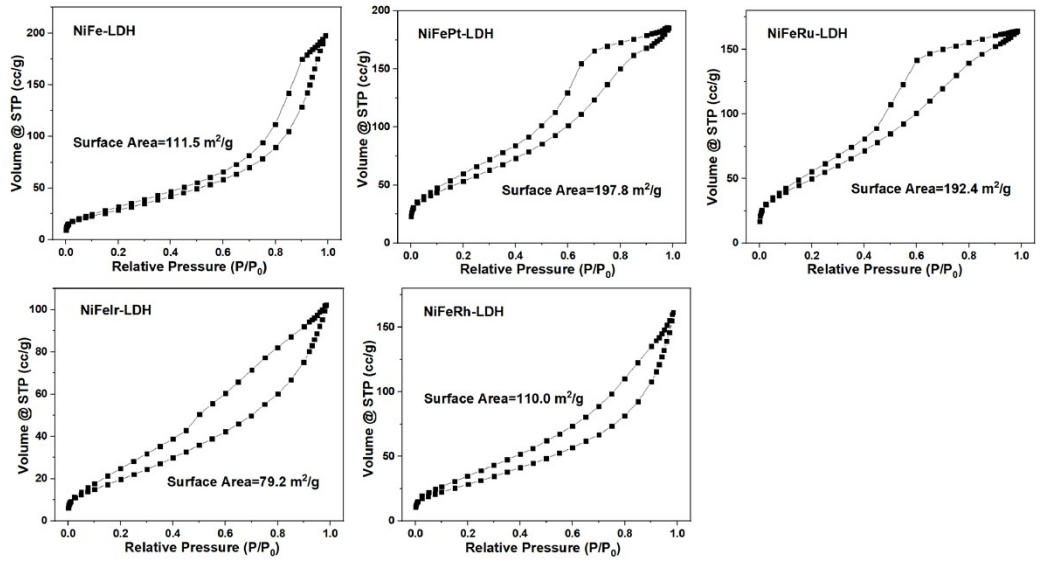

Fig. S1 N_2 adsorption-desorption isotherms and the corresponding surface area of NiFe-LDH and NiFeM-LDH.

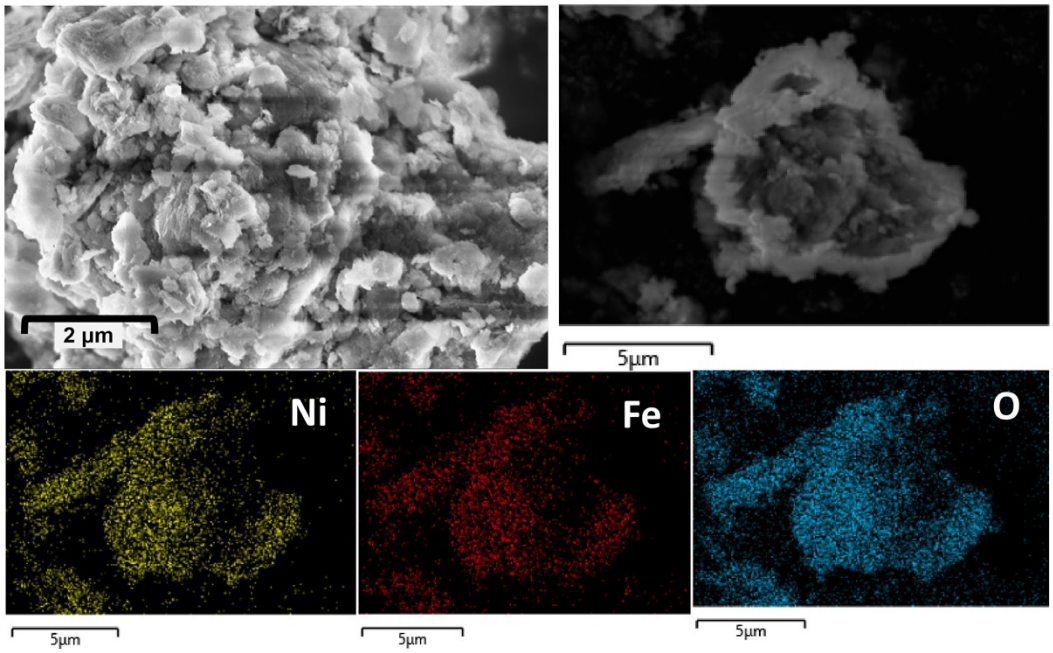

Fig. S2 SEM images and EDS mappings of pristine NiFe-LDH.

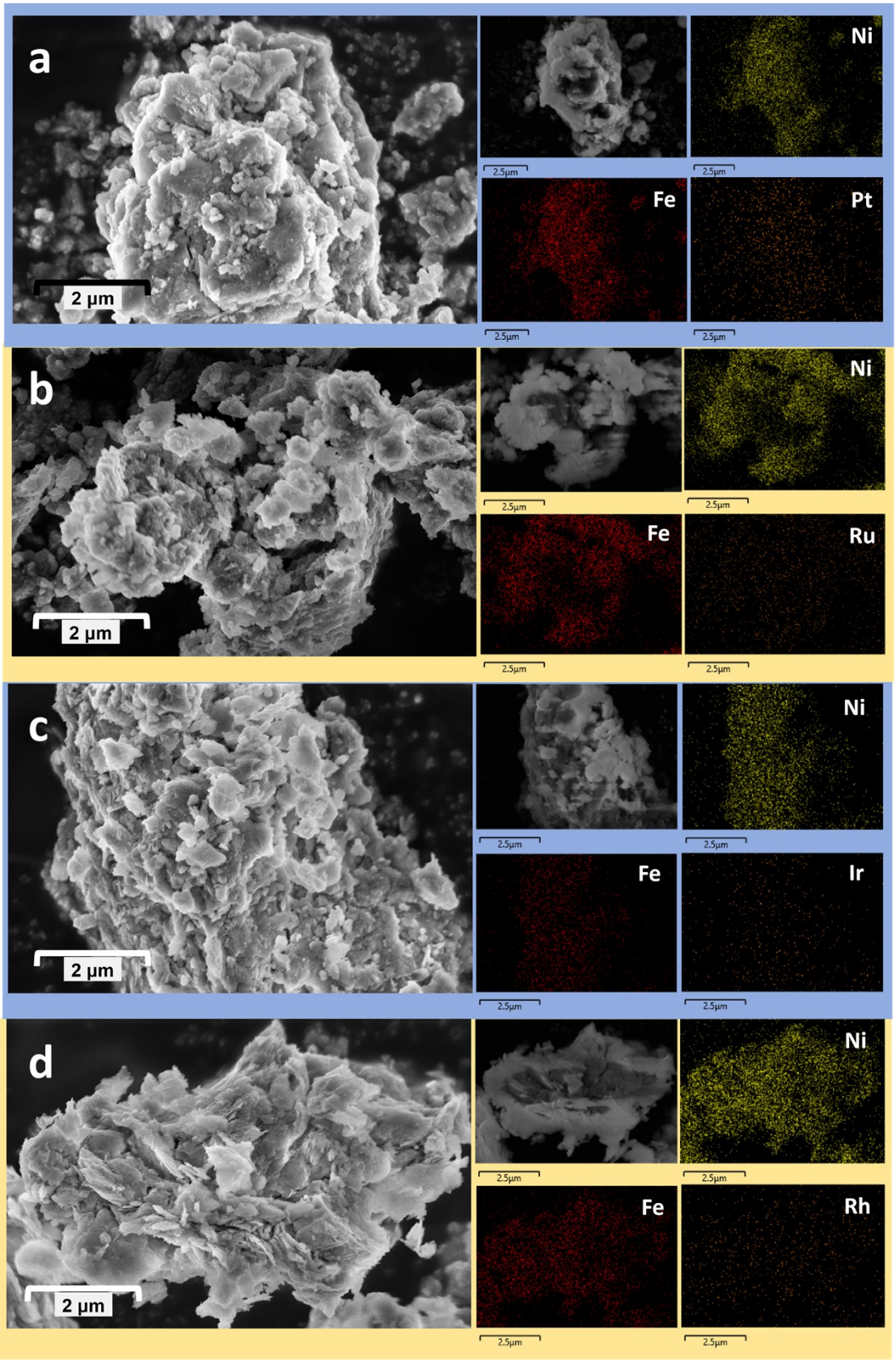

Fig. S3 SEM images and EDS mappings of NiFePt-LDH (a), NiFeRu-LDH (b), NiFeIr-LDH (c), and NiFeRh-LDH (d).

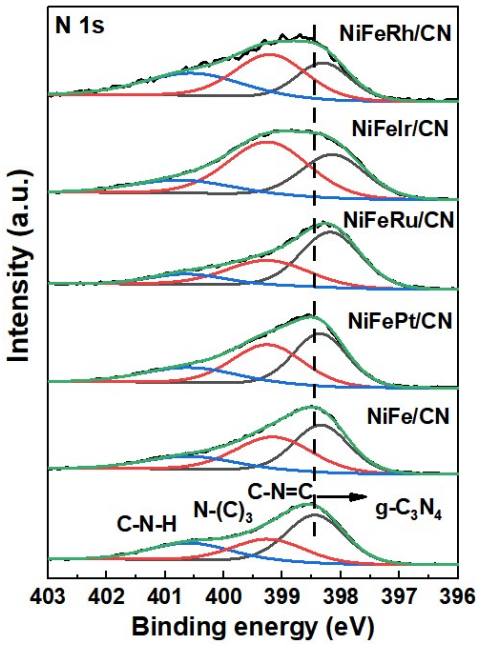

Fig. S4 XPS spectra of N 1s for g-C_3N_4 and NiFeM/CN.

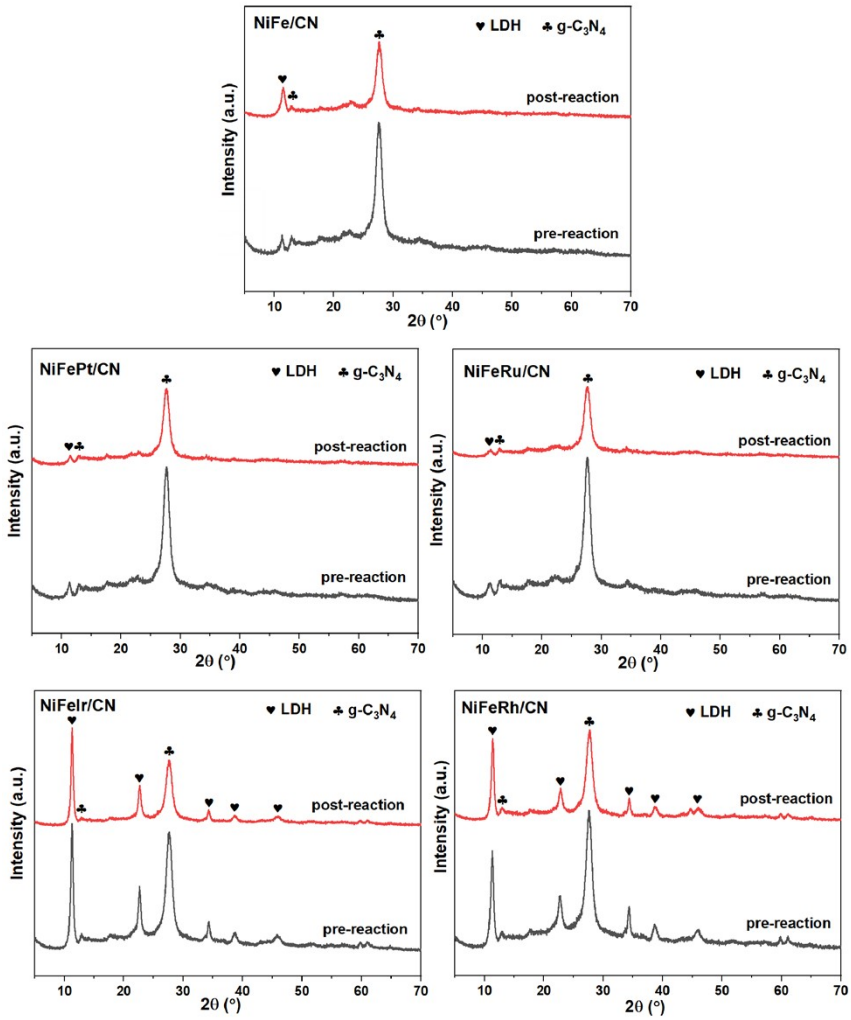

Fig. S5 XRD patterns of NiFe/CN and NiFeM/CN before and after photocatalytic reaction.

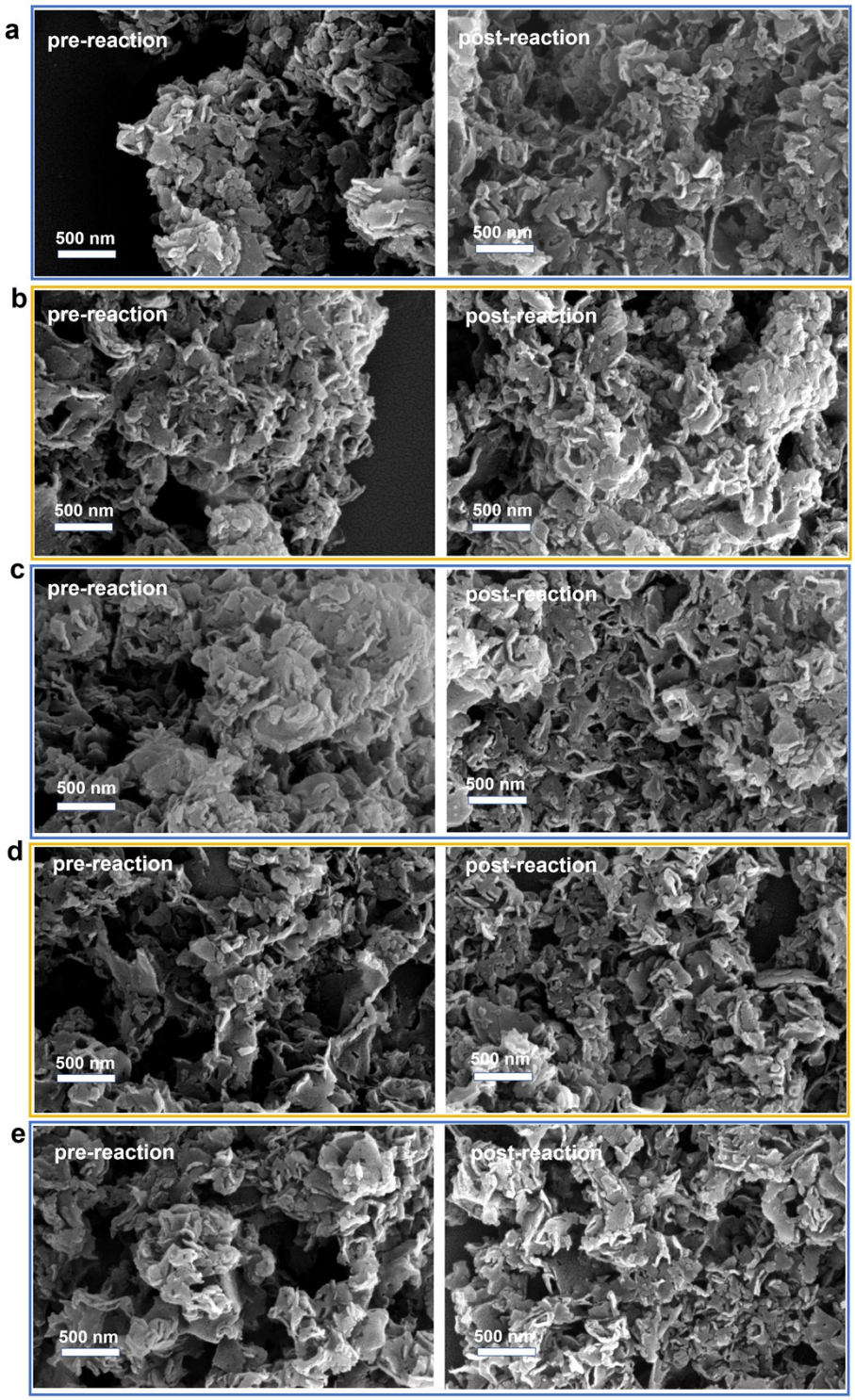

Fig. S6 SEM images of NiFe/CN (a), NiFePt/CN (b), NiFeRu/CN (c), NiFeIr/CN (d) and NiFeRh/CN (e) before and after photocatalytic reaction.

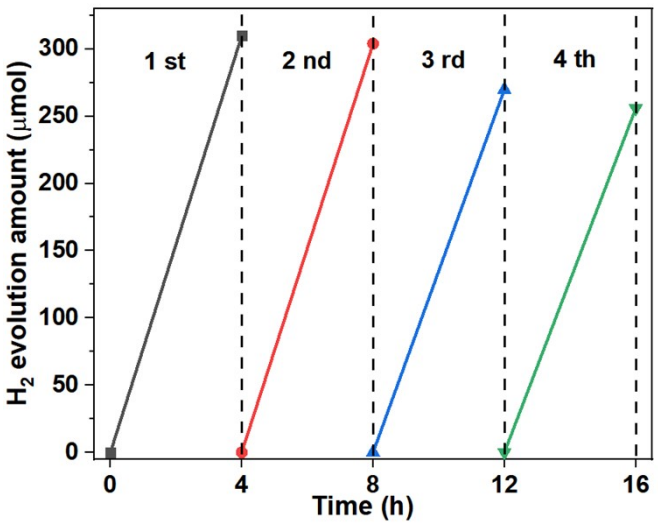

Fig. S7 The stability test of NiFeRu/CN for photocatalytic H_2 evolution (four cycles).

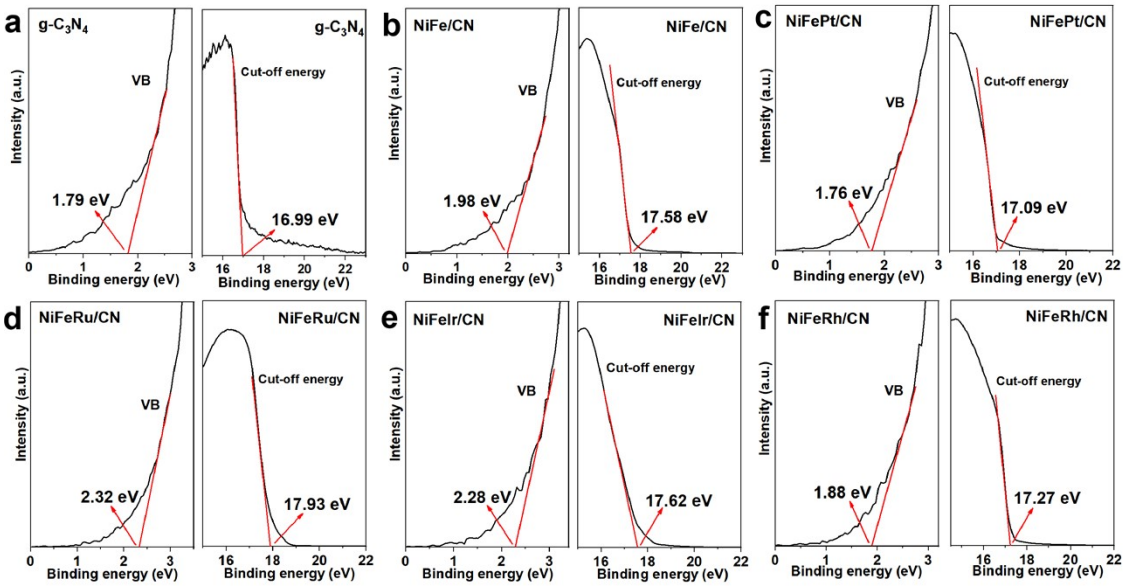

Fig. S8 UPS spectra of g-C_3N_4, NiFe/CN and MiFeM/CN. Note: For semiconductors, the ionization energy (IE) is the energy difference between vacuum level (E_{vac}) and valence band (E_{VB}, or HOMO level). Based on the UPS data, the IE can be calculated by the following formula: IE=hv-($E_{cut-off}$ - E_{VB}), where hv is about 21.22 eV. Then the E_{VB} vs. NHE is calculated as follows: E_{VB} (vs. NHE)= -4.5 eV-E_{VB} (vs. vacuum level), where the E_{VB} (vs. vacuum level) is equivalent to -IE.

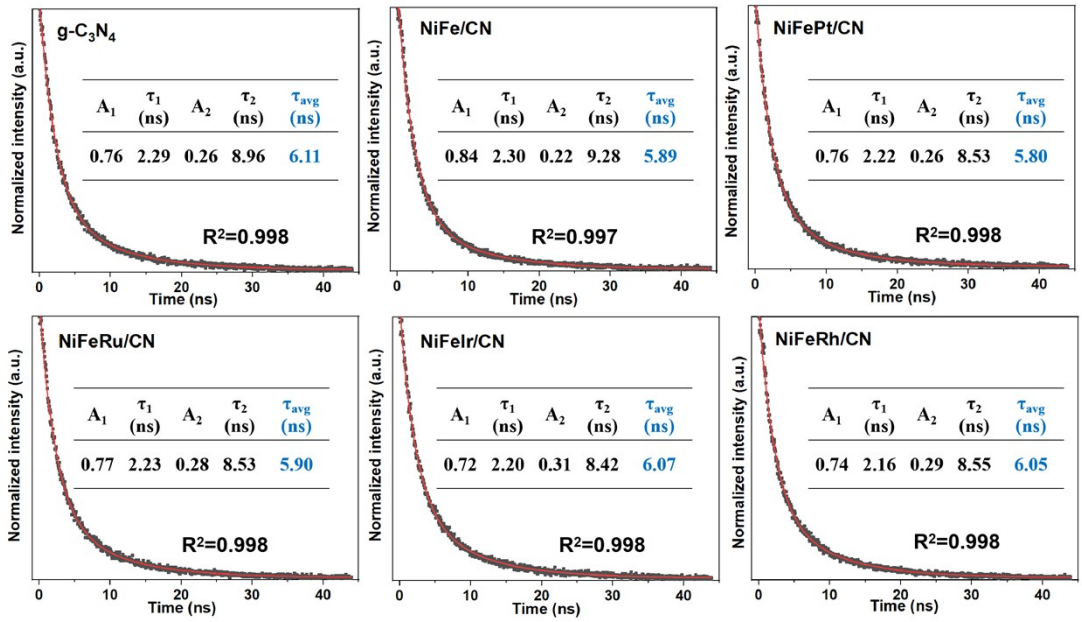

Fig. S9 Time-resolved transient PL decay curves of g-C_3N_4, NiFe/CN and NiFeM/CN, where the spectra were fitted by a two-exponential function: I (t) = $A_1\exp(-t/\tau_1) + A_2\exp(-t/\tau_2)$, $\tau_{avg} = (A_1\tau_1^2 + A_2\tau_2^2) / (A_1\tau_1 + A_2\tau_2)$.

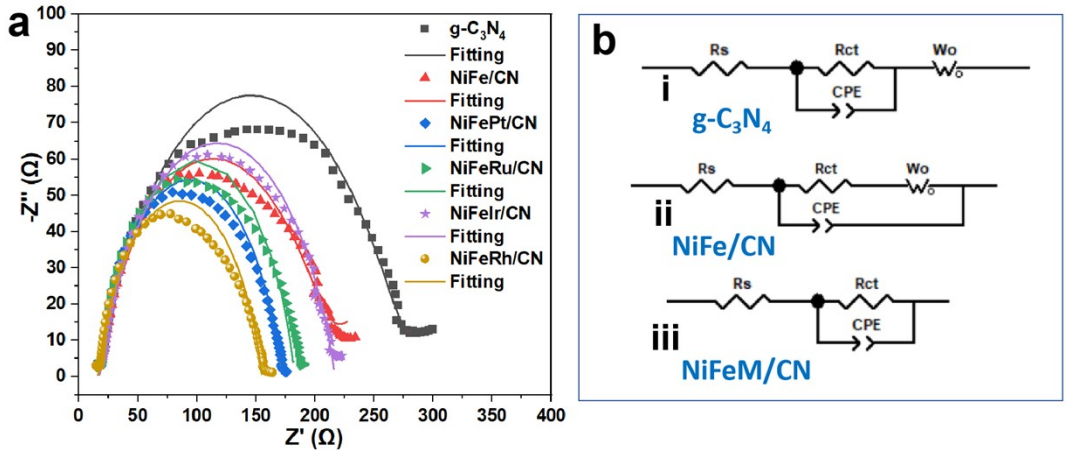

Fig. S10 The measured (symbols) and fitted (solid lines) Nyquist impedance results of pristine g-C_3N_4, NiFe/CN, and NiFeM/CN (a); the corresponding equivalent circuits for fitting (b), i, ii, and iii is for g-C_3N_4, NiFe/CN, and NiFeM/CN, respectively.

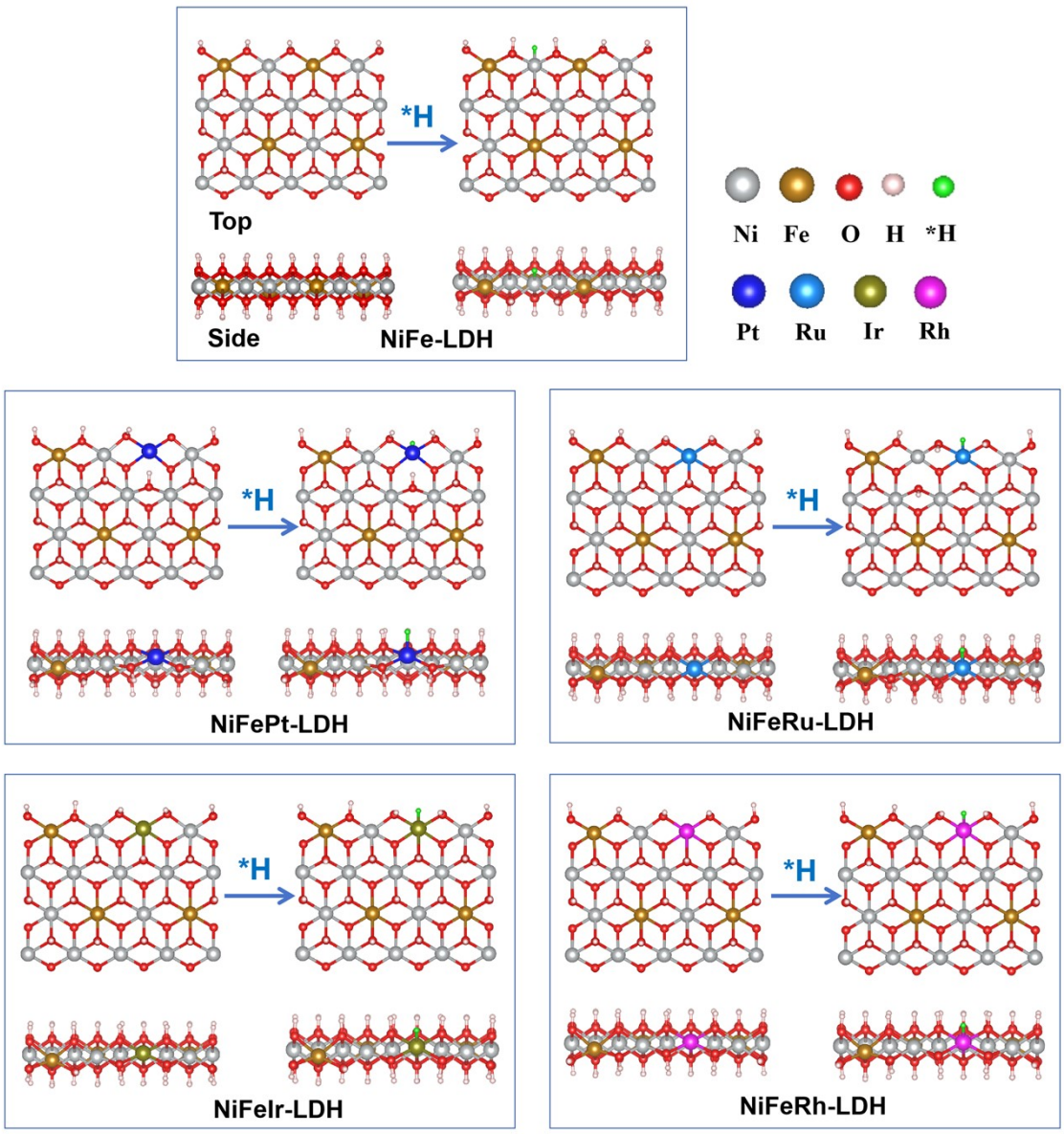

Fig. S11 The geometric configurations of NiFe-LDH and NiFeM-LDH, and the corresponding transition states of H adsorption on Ni site (NiFe-LDH) and noble metal sites (NiFeM-LDH).

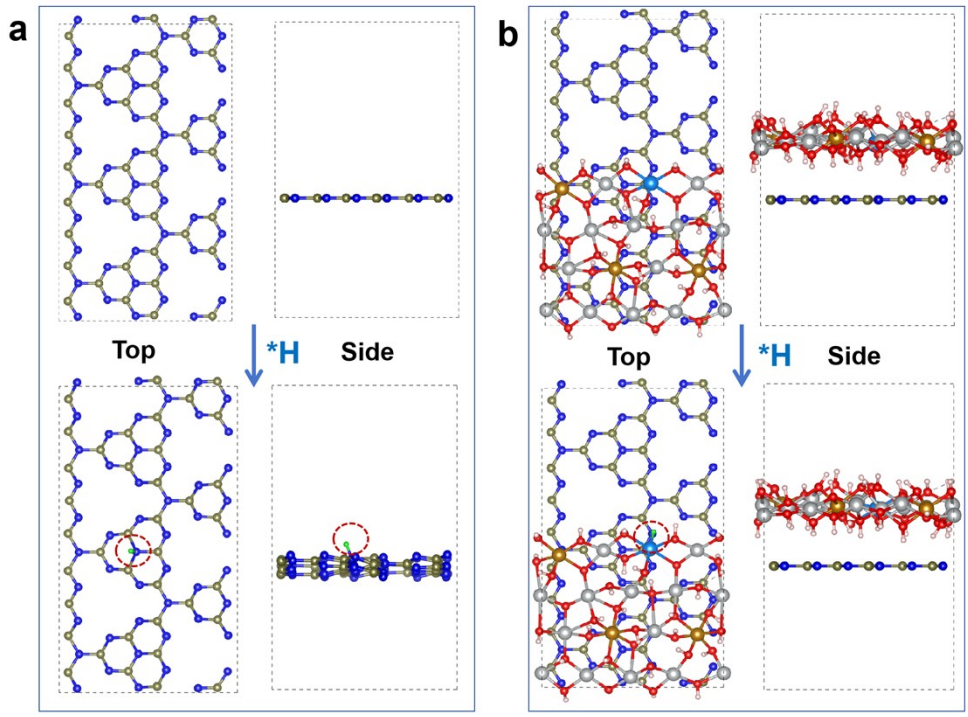

Fig. S12 The geometric configurations and the transition states of H adsorption of g-C_3N_4 (a) and NiFeRu/CN (b).

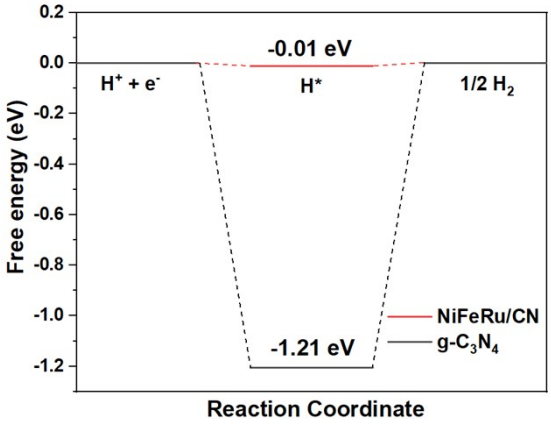

Fig. S13 The calculated free-energy (ΔG_{H^*}) of g-C_3N_4 and NiFeRu/CN.

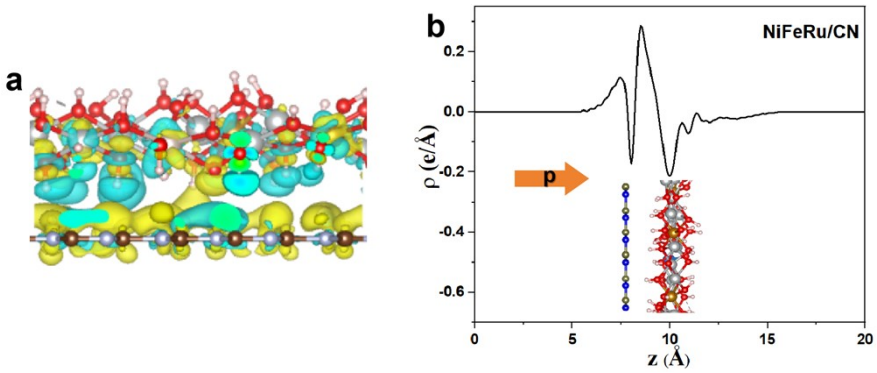

Fig. S14 The charge density difference of NiFeRu/CN, in which blue and yellow regions indicate electron depletion and accumulation, respectively (a); Plane-average charge density difference (b).

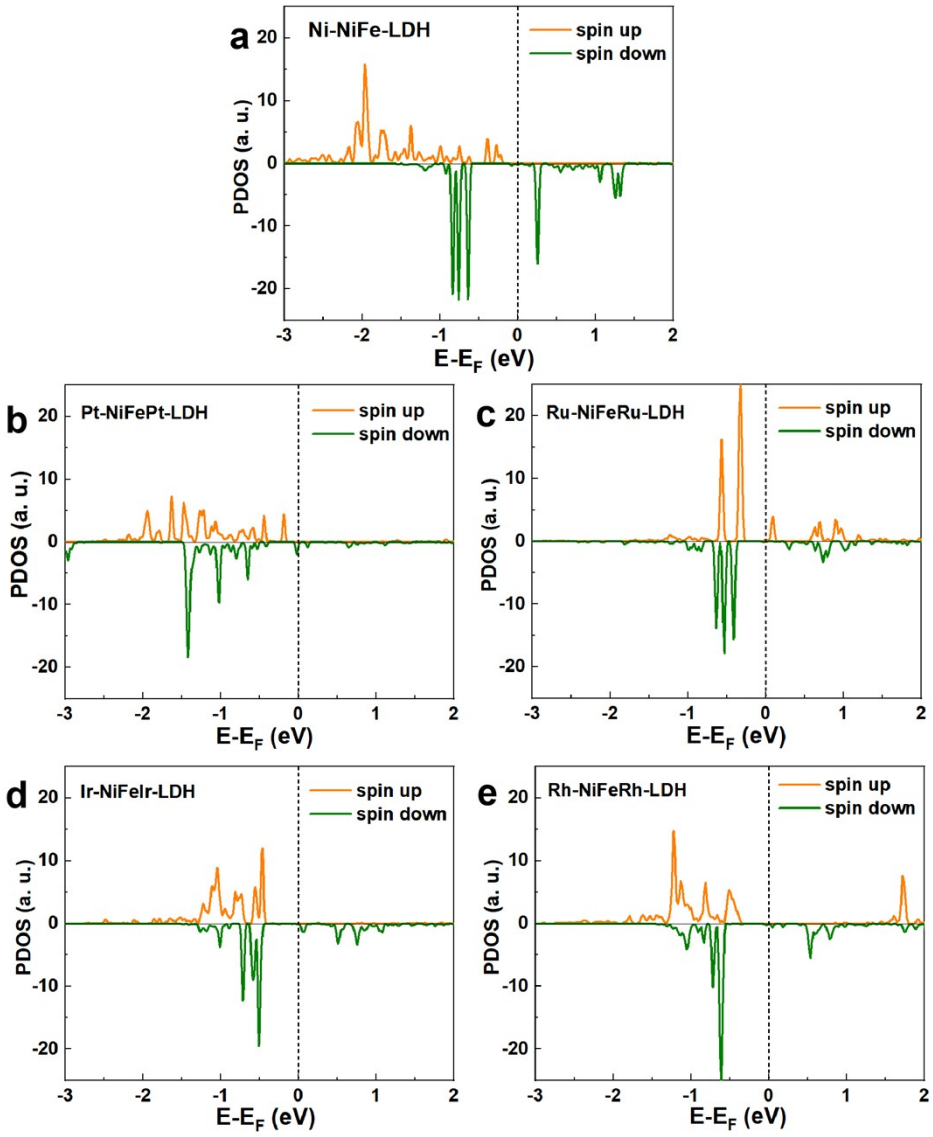

Fig. S15 The partial density of states (PDOS) for Ni in NiFe-LDH (a), Pt in NiFePt-LDH (b), Ru in NiFeRu-LDH (c), Ir in NiFeIr-LDH (d), and Rh in NiFeRh-LDH (e), the E_F corresponds to Fermi level.

Table S1. Surface element content of cocatalysts obtained from EDS analysis

Sample	Element content (wt%)				
	C	O	Ni	Fe	M
NiFe-LDH	57.23	21.41	10.74	10.62	--
NiFePt-LDH	59.13	18.86	8.82	12.64	0.56 (Pt)
NiFeRu-LDH	34.19	25.94	20.79	18.12	0.97 (Ru)
NiFeIr-LDH	46.12	24.84	16.97	11.69	0.38 (Ir)
NiFeRh-LDH	47.83	24.22	15.54	12.16	0.25 (Rh)

Table S2. The fitting parameters for equivalent circuit

Sample	R_s (Ω)	Error of R_s (%)	R_{ct} (Ω)	Error of R_{ct} (%)
g-C_3N_4	14.7	1.16	251.1	0.88
NiFe/CN	16.4	1.17	186.2	6.80
NiFePt/CN	16.9	1.06	155.0	0.91
NiFeRuCN	17.4	1.55	165.7	1.29
NiFeIr/CN	17.7	1.05	199.5	0.90
NiFeRh/CN	16.0	1.07	139.3	0.91

Table S3. Band structures of g-C_3N_4, NiFe/CN and NiFeM/CN

Samples	Band gap	Conduction band (LOMO)	Valence band (HOMO)
g-C_3N_4	2.76 eV	-1.24 eV	1.52 eV
NiFe/CN	2.61 eV	-1.49 eV	1.12 eV
NiFePt/CN	2.66 eV	-1.27 eV	1.39 eV
NiFeRu/CN	2.71 eV	-1.60 eV	1.11 eV
NiFeIr/CN	2.71 eV	-1.33 eV	1.38 eV
NiFeRh/CN	2.71 eV	-1.38 eV	1.33 eV

Note: the band gaps (E_g) are acquired from UV-vis DRS spectra through the formula: E_g (eV)=1240/λ, where λ is related to the absorption edges. And the E_{VB} (vs. NHE) values are acquired from UPS results, E_{CB} (vs. NHE)=E_{VB} (vs. NHE)-E_g.

Table S4. The calculated ΔG_{H^*} on different metal sites

Sample	Ni-H[a]/eV	M-H[c]/eV
NiFe-LDH	**0.58**	0.70[b]
NiFePt-LDH	0.42	**0.26**
NiFeRu-LDH	0.57	**0.19**
NiFeIr-LDH	1.54	**-1.07**
NiFeRh-LDH	2.43	**-0.62**

[a] H adsorption on Ni site. [b] H adsorption on Fe site. [c] H adsorption on doped noble metal sites.

Table S5. The comparison of photocatalytic HER activity of recently reported g-C_3N_4 with cocatalyst loading

Photocatalyst	Cocatalyst	Light source	Reaction conditions	H_2 evolution rate (μmol/h)	AQE	Ref.
NiFeRu/CN	NiFeRu-LDH	300 W Xe lamp	15 mg catalyst, TEOA solution	77.4	0.53% at 420 nm	This work
NiFePt/CN	NiFePt-LDH,	300 W Xe lamp	15 mg catalyst, TEOA solution	43.5	-	This work
Pt/C_3N_4	Pt	300 W Xe lamp	100 mg catalyst, TEOA solution	10.7	0.1% at 420 nm	7
Cu-Ni$(OH)_2$/C_3N_4	Cu-Ni$(OH)_2$	300 W Xe lamp	20 mg catalyst, TEOA solution	40.7	N/A	8
PtNi/C_3N_4	PtNi	300 W Xe lamp	25 mg catalyst, TEOA solution	238.2	10.6% at 370 nm	9
NiCoP/C_3N_4	NiCoP	300 W Xe lamp	60 mg catalyst, TEOA solution	477.1	N/A	10
B-MoS_2/C_3N_4	B-MoS_2	300 W Xe lamp	25 mg catalyst, TEOA solution	40.3	5.54% at 370 nm	11
MoC-Mo_2C/C_3N_4	MoC-Mo_2C	300 W Xe lamp	20 mg catalyst, TEOA solution	81.6	1.3% at 420 nm	12
MoO_2-Pt/C_3N_4	MoO_2-Pt	300 W Xe lamp	50 mg catalyst, TEOA solution	190.2	N/A	13
CoP/CoO/C_3N_4	CoP/CoO	300 W Xe lamp	50 mg catalyst, TEOA solution	43	1.3% at 420 nm	14
Ru-MoS_2/C_3N_4	Ru-MoS_2	300 W Xe lamp	10 mg catalyst, TEOA solution	111.2	N/A	15

Reference

1 G. Kresse and J. Hafner, *Phys. Rev. B Condens.*, 1993, **47**, 558-561.

2 G. Kresse and J. Furthmiiller, *Comput. Mater. Sci.*, 1996, **6**, 15-50.

3 P. E. Blochl, *Phys. Rev. B Condens.*, 1994, **50**, 17953-17979.

4 G. Kresse and D. Joubert, *Phys. Rev. B Condens.*, 1999, **59**, 1758-1775.

5 J. P. Perdew, K. Burke and M. Ernzerhof, *Phys. Rev. Lett.*, 1996, **77**, 3865-3868.

6 S. Grimme, J. Antony, S. Ehrlich and H. Krieg, *J. Chem. Phys.*, 2010, **132**, 154104.

7 X. Wang, K. Maeda, A. Thomas, K. Takanabe, G. Xin, J.M. Carlsson, K. Domen and M. Antonietti, *Nat. Mater.*, 2009, **8**, 76-80.

8 D. Zhan, J. Tian, Q. Fu, P. Liu, Y. Zhao, W. Liu, D. Li, Y. Huang and C. Han, *Appl. Surf. Sci.*, 2023, **641**, 158463.

9 R. Li, Y. Wang, C. Zuo, J. Wang, X. Sheng, Y. Huang, Y. Zhang and Y. Zhou, *Int. J. Hydrogen Energy*, 2023, **48**, 28277-28288.

10 Y. Chen, J, Ma, J. Fu, L. Sun, J. Cheng and J.-F. Li, *Int. J. Hydrogen Energy*, 2024, **51**, 1145-1152.

11 P. Qiu, Y. An, X. Wang, S. An, X. Zhang, J. Tian and W. Zhu, *Chin. Chem. Lett.*, 2023, **34**, 108246.

12 X.-Q. Tan, P. Zhang, B. Chen, A. R. Mohamed and W.-J. Ong, *J. Colloid Interface Sci.*, 2024, **662**, 870-882.

13 F. Su, Z. Wang, M. Tian, C. Yang, H. Xie, C. Ding, X. Jin, J. Chen and L. Ye, *Chem. Asian J.*, 2023, **18**, e202201139.

14 Q. Wang, L. Kong, J. Xu, B. Zhou, X. Liu, Z. Lin, S. Shi, X. Zhang and L. Li, *ACS Sustainable Chem. Eng.*, 2024, **12**, 11717-11727.

15 X. Han, Q. Liu, A. Qian, L. Ye, X. Pu, J. Liu, X. Jia, R. Wang, F. Ju, H. Sun, J. Zhao and H. Ling, *ACS Appl. Mater. Interfaces*, 2023, **15**, 22, 26670-26681.